

Spin- and Charge Excitations of the Triangular Hubbard-Model: a FLEX-Study

Marcus Renner* and Wolfram Brenig

Technische Universität Braunschweig, Institut für Theoretische Physik, Mendelssohnstr. 3, 38106 Braunschweig

(Dated: 29th October 2019)

A study of the quasi-particle excitations and spin fluctuations in the one-band Hubbard-model on the triangular lattice with nearest- and next-nearest-neighbor hopping is presented. Using the fluctuation-exchange-approximation (FLEX) results for the quasi-particle dispersion and life-time, the Fermi surface, and the static spin structure factor will be discussed for a wide range of dopings and as a function of the Coulomb correlation strength U . It is shown that the renormalization of the spin- and charge-dynamics is sensitive to the interplay between van Hove singularity-effects and the nesting, which is influenced by the next-nearest-neighbor hopping. For all dopings investigated, the energy-dependence of the quasi-particle life time is found to be of conventional Fermi-liquid nature. At intermediate correlation strength the static structure factor is strongly doping dependent, with a large commensurate peak at the K -point for 1.35 electrons per site and weak, incommensurate intensities occurring at lower electron densities. The relevance of this model to the recently discovered cobaltates $\text{Na}_x\text{CoO}_2 \cdot y\text{H}_2\text{O}$ will be discussed.

PACS numbers: 71.10.Fd, 71.27.+a, 74.20.Mn, 71.28.+d

Keywords: triangular lattice, Hubbard model, FLEX approximation, spin fluctuations

I. INTRODUCTION

Recent discovery of superconductivity in the cobaltate $\text{Na}_x\text{CoO}_2 \cdot y\text{H}_2\text{O}$, $x \approx 0.35$ with a critical temperature of $T_c \sim 5\text{K}$ ¹ has attracted enormous attention to this material, stimulating a large number of experimental^{2,3,4,5} and theoretical investigations^{6,7,8,9,10,11,12,13,14,15,16}. $\text{Na}_x\text{CoO}_2 \cdot y\text{H}_2\text{O}$ is of space group $\text{P6}_3/\text{mmc}$, representing a hexagonal layered structure which consists of two-dimensional (2D) CoO_2 conduction planes, separated by H_2O and Na^+ ions. The material is derived from its parent compound NaCo_2O_4 , equivalent to $x=0.5$, by simultaneous intercalation of H_2O and deintercalation of Na^+ ions. This process nearly doubles the c -axis lattice-constant, strongly enhancing the 2D character of the compound. The Co ions form a *triangular* lattice and are coordinated by edge-sharing oxygen-octahedra which display a shift of the oxygen atoms along the $(1,1,1)$ -direction. In this environment the low-lying t_{2g} -manifold splits into a non-degenerate A_{1g} level and an E_g -doublet, leaving Co^{4+} in a low-spin, $S=1/2$ state, with a single electron in the A_{1g} level while Co^{3+} has a filled A_{1g} orbital¹⁷. In turn, x can be viewed as *electron doping* away from half-filling of a non-degenerate one-band model on a triangular lattice, with $\text{Na}_x\text{CoO}_2 \cdot y\text{H}_2\text{O}$, $x \approx 0.35$ referring to an electron density of $n \approx 1.35$ per site.

At present, the electronic structure of the cobaltates is an open issue. Yet, there is a tempting similarity to the high-temperature superconducting cuprates, where however d -holes are arranged on a 2D *square*-lattice. Early on, the role of electron correlations in the cobaltates has been of interest. LDA results in an A_{1g} bandwidth of $W \approx 1.4\text{eV}$, while the d -shell Coulomb-correlation strength U is of order 5-8eV typically¹⁷. Motivated by this, resonating-valence-bond (RVB)^{18,19} scenarios have been pursued by several researchers^{6,7,8,12,14}. In addition,

weak-coupling calculations, using renormalization-group (RG) methods have also been performed⁹. In this paper we apply an alternative method, suitable for intermediate correlation strength, namely the fluctuation-exchange-approximation (FLEX)^{20,21} and investigate the spin- and charge-dynamics in the triangular Hubbard-model. In passing, we note that such analysis may also shed light onto the organic superconductors $\kappa\text{-(ET)}_2\text{X}$ ²². These have been suggested to realize the Hubbard-model on an *anisotropic* triangular lattice²².

The paper is organized as follows: in section II we discuss the model and briefly review the FLEX method. In section III results for the renormalized dispersions, Fermi surfaces, the static spin structure factor, and the frequency dependence of the selfenergy are discussed for several dopings.

II. MODEL AND METHOD

Our subsequent analysis is focussed on the normal state properties of the one-band Hubbard-model on the triangular lattice

$$H = - \sum_{ij} t_{ij} (c_i^\dagger c_j + h.c.) + U \sum_i n_{i\uparrow} n_{i\downarrow}. \quad (1)$$

Due to the lack of electron-hole symmetry, a choice has to be made to fix the sign of the hopping matrix elements t_{ij} and the Coulomb repulsion U . Here we fix these parameters to model the electronic structure of $\text{Na}_x\text{CoO}_2 \cdot y\text{H}_2\text{O}$ which we assume to be similar to the one of the parent compound. LDA calculations on NaCo_2O_4 ¹⁷ place the Fermi energy in a CEF-split t_{2g} manifold of Co d -bands with the states near the Fermi energy E_F to be of a_{1g} symmetry. Due to a weak unit-cell doubling a 'bilayer'-type splitting exists which

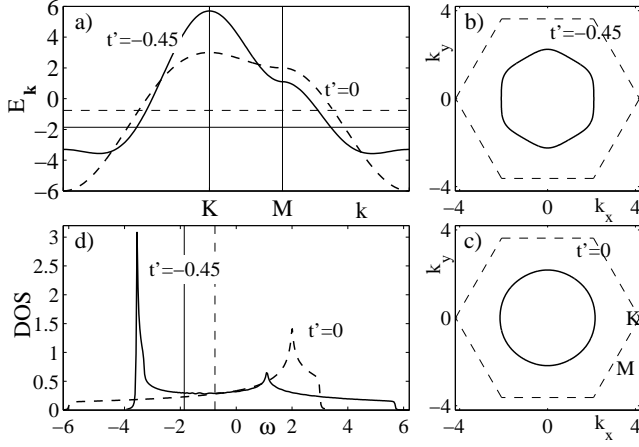


Figure 1: a) dispersion, b), c) Fermi surface, and d) density of states for the tight-binding energy of eqn. (2) for $t' = 0$ versus $t' \neq 0$. In a) [d)] horizontal[vertical] solid(dashed) lines refer to chemical potentials μ at $n = 0.65$. In b) and c) dashed hexagons label Brillouin zone of triangular lattice.

we will neglect henceforth. LDA finds the maximum of the a_{1g} - t_{2g} bands at the Γ -point. Focussing at first on the nearest-neighbor(n.n.)-hopping $t = t_{\langle ij \rangle}$, and using an electron-language this implies that $t > 0$ in eqn. (1). Coulomb-correlations however, suppress double occupancy of the a_{1g} - t_{2g} level by holes. Therefore, for the remainder of this paper we switch to the hole-language, implying $t > 0$ and $U > 0$. The corresponding tight-binding band and bare DOS, as well as the Fermi surface (FS) and chemical potential for $n \approx 0.65$ are shown in Fig. 1. In the remainder of this paper all energies will be expressed in units of t .

Next, it is important to realize that a dispersion with n.n.-hopping only is *qualitatively* different from the LDA. First, the latter exhibits a pronounced dip at the Γ -point. Second, the LDA FS for the parent compound NaCo_2O_4 , i.e. at $n=0.5$, is notably hexagonal, while the tight-binding FS using n.n.-hopping only is practically circular at this doping. These facts signal a sizeable next-nearest-neighbor(n.n.n.) hopping $t' = t_{\langle\langle ij \rangle\rangle}$ in the cobaltates. Fitting the corresponding dispersion

$$\epsilon_{\mathbf{k}} = -2t(\cos(k_x) + 2\cos(k_x/2)\cos(\sqrt{3}k_y/2)) - 2t'(2\cos(3k_x/2)\cos(\sqrt{3}k_y/2) + \cos(\sqrt{3}k_y)) \quad (2)$$

to the LDA along the Γ - M direction we find $t' \approx -0.45$. As can be read of from Fig. 1 this does not only lead to the required dip in the dispersion and the hexagonal FS shape, but also to a signature of van Hove singularities very different from the case $t' = 0$. For $t' = 0$ the bandwidth is $W = 9$, while for $t' = -0.45$ it is slightly increased to 9.26. The role of n.n.n. hopping has also been emphasized in a recent search for possible f -wave SC²³ using third order perturbation in U/t for the gap

equation, which is rather different from the approach presented here.

To study the model (1,2) we employ the diagrammatic FLEX approximation²⁰. The FLEX is conserving in the sense of Kadanoff and Baym²⁴. It sums all particle-hole(particle) ladder-graphs for the generating functional selfconsistently and it is believed to apply up to intermediate correlation strength $U/t \sim 1$. The FLEX equations for the bare(renormalized spin- and charge-) susceptibilities $\chi^0(\chi^{s,c})$, the one-particle Greens function(selfenergy) $G(\Sigma)$, and the effective interaction V read

$$\chi_{\mathbf{q}}^0(\nu_m) = -\frac{T}{N} \sum_{\mathbf{k}, n} G_{\mathbf{k}+\mathbf{q}}(\omega_n + \nu_m) G_{\mathbf{k}}(\omega_n) \quad (3)$$

$$\chi_{\mathbf{q}}^{s,c}(\nu_m) = \chi_{\mathbf{q}}^0(\nu_m) [1 \mp U\chi_{\mathbf{q}}^0(\nu_m)]^{-1} \quad (4)$$

$$V_{\mathbf{q}}(\nu_m) = U^2 \left(\frac{3}{2} \chi_{\mathbf{q}}^s(\nu_m) + \frac{1}{2} \chi_{\mathbf{q}}^c(\nu_m) - \chi_{\mathbf{q}}^0(\nu_m) \right) \quad (5)$$

$$\Sigma_{\mathbf{k}}(\omega_n) = \frac{T}{N} \sum_{\mathbf{k}', n'} V_{\mathbf{k}-\mathbf{k}'}(\omega_n - \omega_{n'}) G_{\mathbf{k}'}(\omega_{n'}) \quad (6)$$

where $\omega_n = i\pi T(2n+1)$ and $\nu_m = i\pi T 2m$. Eqns. (3-6) have to be solved selfconsistently taking into account that $G_{\mathbf{k}}^{-1}(\omega_n) = [\omega_n - \epsilon_{\mathbf{k}} + \mu - \Sigma_{\mathbf{k}}(\omega_n)]^{-1}$. We compute the Matsubara summations using the 'almost real contour' technique of ref.²⁵. I.e., contour integrals are performed with a *finite* shift $i\gamma$ ($0 < \gamma < iT\pi/2$) into the upper half plane. All final results are analytical continued from $\omega + i\gamma$ onto the real axis $\omega + i0^+$ by Padé approximation. The following results are based on FLEX solutions using a lattice of 64×64 sites with 4096 equidistant ω -points in the energy range of $[-30, 30]$. The temperature has been kept at $T = 0.05$.

III. RESULTS AND DISCUSSION

We start the discussion of our results with the quasi-particle dispersion $E_{\mathbf{k}}$ which is determined by $E_{\mathbf{k}} - \epsilon_{\mathbf{k}} + \mu - \Sigma_{\mathbf{k}}(E_{\mathbf{k}}) = 0$. This dispersion is shown in Fig. 2(a) and (b) at $U/W \sim 1$ for $t' = 0$ and -0.45 for various doping levels δ , where $\delta = n - 1$ within the hole-picture, i.e. $\text{Na}_x\text{CoO}_2 \cdot y\text{H}_2\text{O}$ with $x \approx 0.35$ corresponds to $\delta \approx -0.35$. As compared to Fig. 1 (a) a pronounced mass-enhancement of order unity at the FS crossings is clearly visible in Fig. 2 (a) and (b). This enhancement is due to low-energy spin fluctuations which are present in $\chi_{\mathbf{q}}^s(\omega)$. In addition the overall shape of the dispersion is strongly renormalized. At large distances from the FS however, and due to strong quasi-particle scattering, the notion of the quasi-particle pole $E_{\mathbf{k}}$ may be of less relevance.

At $U = 0$, $t' = 0$, and for $\delta = +0.5$ the Fermi energy coincides with the van Hove singularity related to a flattening of the bare dispersion observable in Fig. 1 (a) along Γ - M - K . Fig. 2 (a) shows a shift of this flattening at finite U . Eg. for $U = 8$ we find the Fermi energy to coincide with the remnants of the van Hove singularity

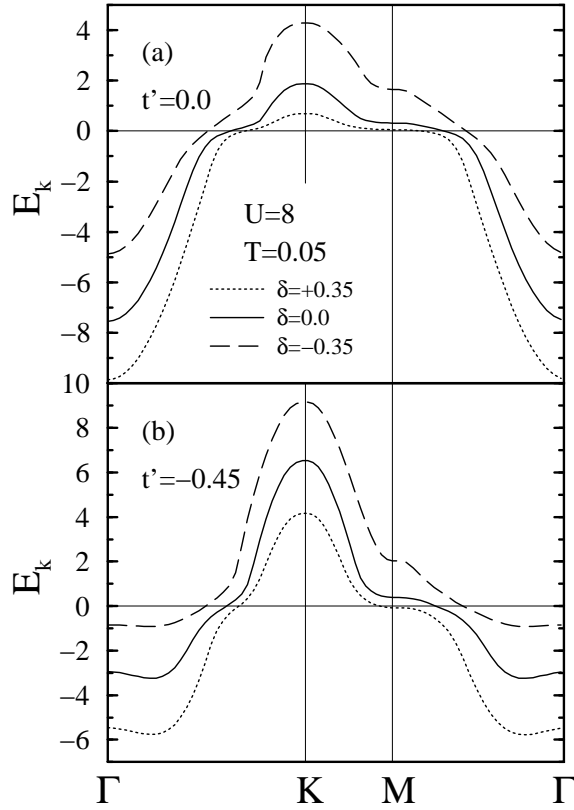


Figure 2: Quasi-particle dispersion $E_{\mathbf{k}}$ along Γ - K - M - Γ for (a) $t' = 0$ and (b) $t' = -0.45$ and for various doping levels at $U = 8$ and $T = 0.05$.

only at $\delta \approx +0.35$. This is rather remote from the SC's doping level. In ref.⁹ Fermi surface pinning of the van Hove singularity has also been investigated, however at fixed chemical potential. For $t' \neq 0$ the situation is very different since *two* van Hove singularities exist in the bare DOS. Remnants of these remain present also at finite U . At $t' = -0.45$ and $U = 8$ Fig. 2 (b) shows that for the SC's doping level of $\delta \approx -0.35$ the FS is rather close to the lower one of the van Hove singularities - which is absent at $t' = 0$. Finally we note from Fig. 2 (a), that for $t' = 0$ the relative mass-enhancement at the FS along directions unrelated to the van Hove singularity, e.g. Γ - K is largest if the van Hove singularity is closest to the FS. For $t' = -0.45$ Fig. 2 (b) does not show this effect.

In Fig. 3 the FS of the t - and $t - t' - U$ models are compared for $\delta = 0, \pm 0.35$. As compared to the non-interacting case at $U = 0$ there are no indications of sizeable, correlation-induced shape-changes of the FS. The FS at finite and negative $t' = -0.45$ is hexagonally shaped for $\delta \leq 0$ down to the SC's doping level. This is consistent with the LDA results of ref.¹⁰. In contrast, the FS at $t' = 0$ evolves towards a more circular shape as $\delta = -0.35$ is reached. Below we will show that nesting of the flat regions of the FS with the wave-vector $\mathbf{Q}(\delta)$ indicated in Fig. 3 enhances the static spin structure factor at $\mathbf{Q}(\delta)$. Due to the shape of the FS this enhancement

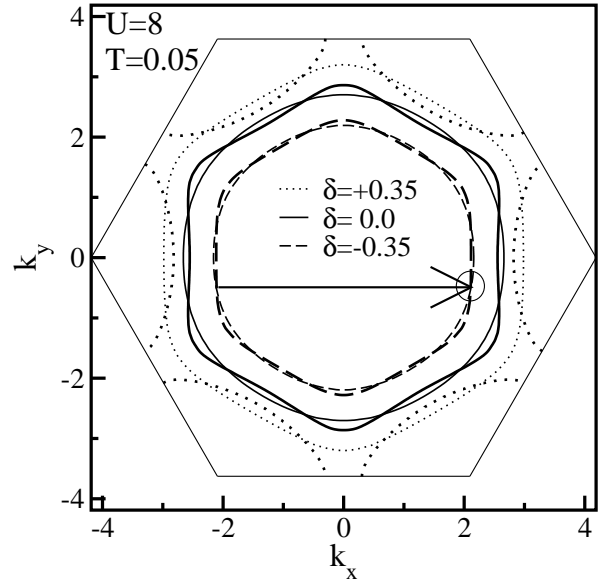


Figure 3: Fermi surfaces for $t' = 0$ (thin lines) versus $t' = -0.45$ (thick lines) at $U = 8$ and $T = 0.05$ for various δ . Outer hexagon refers to BZ. Arrow denotes a commensurate wave vector $\mathbf{K} = (\frac{4\pi}{3}, 0)$ with a circle labeling the half width of $\chi_{\mathbf{q}}^s$ at $\mathbf{q} = \mathbf{K}$ at $T = 0.05$, $U = 8$, and $t' = 0$.

is more pronounced for $t' = -0.45$. Interestingly, at the SC's doping level the nesting-vector \mathbf{Q} is *commensurate*, i.e. $\mathbf{Q}(\delta \approx -0.35) = \mathbf{K} = (\frac{4\pi}{3}, 0)$.

Now, we discuss the evolution of the static spin structure factor $\text{Re}[\chi_{\mathbf{k}}^s(\omega = 0)]$ with dopings δ and correlation strength U along the path Γ - K - M - Γ in momentum space, contrasting the case of $t' = 0$ versus $t' = -0.45$. Fig. 4 displays the doping dependence at $T = 0.05$ and $U = 8$. For $\delta = +0.35$ this figure shows the static structure factor to be only moderately enhanced within a rather broad range of incommensurate momenta. For $t' = 0$ these momenta are located at $\sim 1.4\mathbf{K}$ along Γ - K and Γ - M . These positions correspond to the displacement of the quasi-parallel regions of the hexagonal FS shown in Fig. 3. For $t' = -0.45$ and $\delta = +0.35$ enhanced spin fluctuations are found primarily along the direction Γ - M with an almost isotropic $\text{Re}[\chi_{\mathbf{k}}^s(\omega = 0)]$ within the remaining \mathbf{k} -space. As the doping is reduced the maxima in $\text{Re}[\chi_{\mathbf{k}}^s(\omega = 0)]$ move towards the K -point and develop into a sharp and *commensurate* peak at $\mathbf{Q}(\delta) = \mathbf{K}$ as the SC's doping level of $\delta = -0.35$ is reached. The shoulder at M in Fig. 5 is due to the overlap with the remaining peaks at symmetry equivalent positions. Nearly all incommensurate spin fluctuations are suppressed. The half width of the commensurate spin fluctuation peak for $\delta = -0.35$ and $t' = 0$ is sketched by the circle on the right hand side of the inner FS in Fig. 3. This circle is also a measure for the degree of nesting of the quasi-parallel regions of the Fermi surface. At $\delta = -0.35$, close to the SC's doping level, the commensurate peak is $\sim 60\%$ larger for $t' = -0.45$ than for $t' = 0$. At $\delta = +0.35$ however, where the nesting

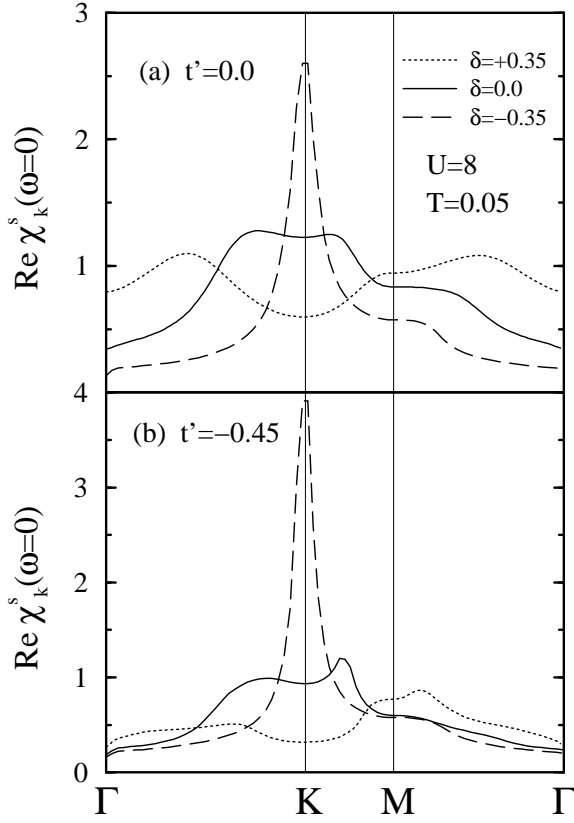


Figure 4: Doping dependence of the static spin structure factor $\text{Re} \chi_{\mathbf{k}}^s(\omega = 0)$ along the path Γ -K-M- Γ in the BZ for (a) $t' = 0$ and (b) $t' = -0.45$. Notice that only at $\delta = -0.35$ the commensurate peak at \mathbf{K} is observed for large U .

properties of the t - and $t - t' - U$ models are rather reversed, the spin response is less suppressed for $t' = 0$.

In Fig. 5 (a) and (b) the dependence of the static spin structure factor on the correlation strength U is displayed at the SC's approximate doping concentration for $t' = 0$ and $t' = -0.45$ along a path in the BZ identical to that of Fig. 4. Evidently, increasing U at this doping level, predominantly increases $\text{Re} [\chi_{\mathbf{k}}^s(\omega = 0)]$ at the commensurate momentum \mathbf{K} . Additionally, one realizes that this increase is non-linear in U , with a rather sizeable growth setting in for $U \gtrsim 4$. Finally, and similar to the doping dependence, the overall size and sensitivity of the spin fluctuations to the correlation strength is larger at $t' = -0.45$ than at $t' = 0$. In contrast to the situation at $\delta = -0.35$ we have found the incommensurate spin fluctuation peaks at $\delta = +0.35$ to be enhanced only weakly with U increasing up to $U = 8$.

Fig. 6 shows the low-temperature frequency dependence of the imaginary part of the quasi-particle self-energy $\text{Im} \Sigma_{\mathbf{k} \in FS}(\omega)$ for $\delta = 0$, and ± 0.35 . The lattice momenta are chosen as close as possible to the FS. We find the selfenergy to be nearly isotropic along the FS with only a rather weak maximum occurring in the direction of the commensurate spin fluctuations. Near the Fermi en-

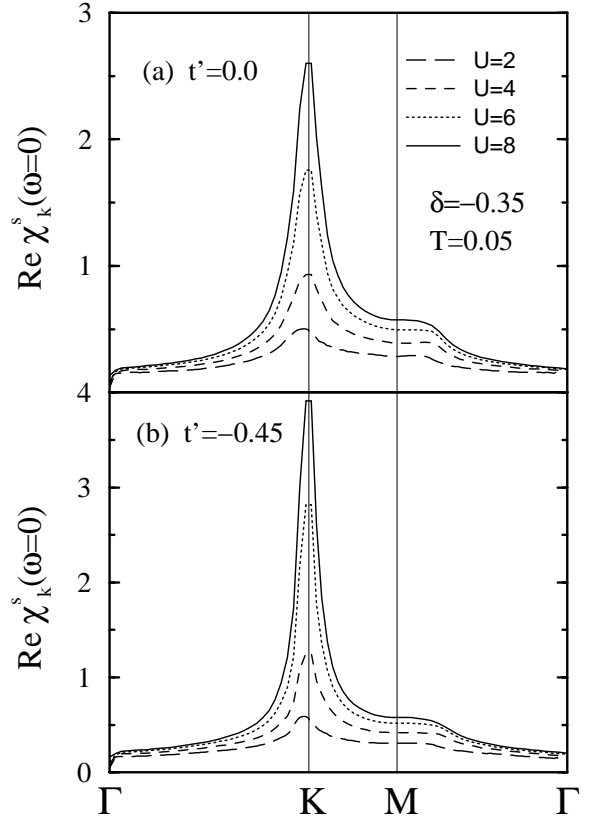


Figure 5: Dependence of the static spin structure factor $\text{Re} \chi_{\mathbf{k}}^s(\omega = 0)$ on the correlation strength U along the path Γ -K-M- Γ in the BZ for (a) $t' = 0$ and (b) $t' = -0.45$.

ergy and for *all* dopings shown, the selfenergy is clearly proportional to ω^2 at low-energies which is indicative of normal Fermi-liquid behavior. This is in sharp contrast to FLEX analysis of the Hubbard-model on the *square lattice*, close to half filling. There one typically finds 'marginal' Fermi-liquid behavior with $\text{Im} \Sigma_{\mathbf{k} \in FS}(\omega) \propto \omega$ over a wide range of frequencies^{21,26}. Therefore, along this line one is tempted to conclude, that the normal state of the cobaltates is more of conventional metallic nature than in the cuprates. This is even more so, if one realizes from Fig. 6 that the quasi-particle scattering rate displays its smallest curvature at the SC's doping level, which implies the quasi-particles to be rather well defined there. At larger values of δ , proximity of the FS to the van Hove singularities enhance both, the absolute value of $\text{Im} \Sigma_{\mathbf{k} \in FS}(\omega)$ as well as the curvature. This effect is more pronounced for $t' = 0$.

In summary we have investigated the one-band Hubbard-model on a triangular lattice with nearest- and next-nearest-neighbor hopping using the normal state version of the FLEX approximation. Adapting this model to the cobaltates we have shown that a sizeable next-nearest-neighbor hopping is necessary to describe their electronic structure. Over a substantial range of dopings which we have investigated we find a significant

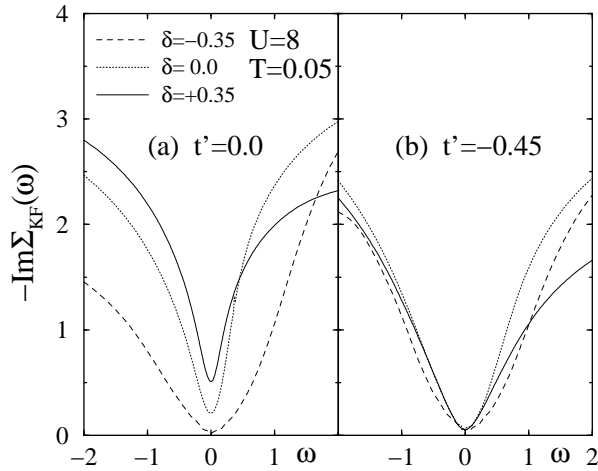


Figure 6: Frequency dependence of $-\text{Im}\Sigma_{\mathbf{k}}(\omega)$ near the FS in direction $\Gamma \rightarrow K$ for (a) $t' = 0$ and (b) $t' = -0.45$ and $\delta = 0, \pm 0.35$ (location of momenta \mathbf{k} in units of \mathbf{K} for (a): $\delta = -0.35$: $33/64$; $\delta = 0.0$: $42/64$; $\delta = +0.35$: $45/64$ and (b): $\delta = -0.35$: $33/64$; $\delta = 0.0$: $39/64$; $\delta = +0.35$: $42/64$).

Fermi surface mass-enhancement of order unity. This is due to spin fluctuations and the additional proximity of the Fermi surface to van Hove singularities at particular doping levels. In contrast to the Hubbard-model on the square-lattice we have found the quasi-particle scattering rate to display a conventional Fermi-liquid type of energy-dependence. Finally we have shown that the static spin structure factor exhibits a large commensurate peak at those doping levels attributed to the superconducting cobaltate systems. This response was found to be significantly enhanced by next-nearest-neighbor hopping.

* Electronic address: m.renner@tu-braunschweig.de

- ¹ K. Takada et al., *nature* **422**, 53 (2003).
- ² B. Lorenz et al., *Phys. Rev. B* **68**, 132504 (2003).
- ³ R. E. Schaak et al., *nature* **424**, 527 (2003).
- ⁴ H. Sakurai et al., *cond-mat/0304503* (2003).
- ⁵ M. Z. Hasan et al., *cond-mat/0308438* (2003).
- ⁶ G. Baskaran, *Phys. Rev. Lett.* **91**, 097003 (2003).
- ⁷ B. Kumar and B. S. Shastry, *cond-mat/0304210* (2003).
- ⁸ Q.-H. Wang, D.-H. Lee, and P. A. Lee, *cond-mat/0304377* (2003).
- ⁹ C. Honerkamp, *Phys. Rev. B* **68**, 104510 (2003).
- ¹⁰ D. J. Singh, *Phys. Rev. B* **68**, 020503 (2003).
- ¹¹ A. Tanaka and X. Hu, *cond-mat/0304409* (2003).
- ¹² M. Ogata, *cond-mat/0304405* (2003).
- ¹³ Q.-H. Wang and Z. D. Wang, *cond-mat/0305152* (2003).
- ¹⁴ T. Li and Y.-J. Jiang, *cond-mat/0309275* (2003).
- ¹⁵ L.-J. Zou, J.-L. Wang, and Z. Zeng, *cond-mat/0307560* (2003).
- ¹⁶ J. Kunes, K.-W. Lee, and W. E. Pickett,

cond-mat/0308388 (2003).

- ¹⁷ D. J. Singh, *Phys. Rev. B* **61**, 13397 (2000).
- ¹⁸ P. W. Anderson, *Mat. Res. Bull.* **8**, 153 (1973).
- ¹⁹ P. Fazekas and P. W. Anderson, *Phil. Mag.* **30**, 423 (1974).
- ²⁰ N. E. Bickers, D. J. Scalapino, and S. R. White, *Phys. Rev. Lett.* **62**, 961 (1989).
- ²¹ J. Altmann, W. Brenig, and A. P. Kampf, *Eur. Phys. J. B* **18**, 429 (2000).
- ²² For recent reviews of κ -(ET)₂X see M. Lang and J. Müller, *cond-mat/0302157v1* (2003) and J. Singleton and Ch. Mielke, *Contemporary Physics* **43** (2002).
- ²³ I. Ikeda, Y. Nisikawa, and K. Yamada, *cond-mat/0308472* (2003).
- ²⁴ G. Baym, *Phys. Rev.* **127**, 1391 (1962).
- ²⁵ J. Schmalian et al., *Computer Phys. Comm.* **93**, 141 (1996).
- ²⁶ S. Wermbter, *Phys. Rev. B* **55**, R10149 (1997).